Journal of Biomechanics 45 (2012) 1112–1116

Contents lists available at SciVerse ScienceDirect

Journal of Biomechanics

journal homepage: www.elsevier.com/locate/jbiomech
www.JBiomech.com

Short communication

Comparison of different camera calibration approaches for underwater applications

Amanda Piaia Silvatti [a,c,*], Fabio Augusto Salve Dias [b], Pietro Cerveri [c], Ricardo M.L. Barros [a]

[a] Faculty of Physical Education–University of Campinas, SP, Brazil
[b] Laboratoire d'Informatique Gaspard-Monge, ESIEE, Paris, France
[c] Biomedical Engineering Department–Politecnico di Milano, MI, Italy

ARTICLE INFO

Article history:
Accepted 1 January 2012

Keywords:
Camera calibration
3D underwater analysis
Sports and rehabilitation

ABSTRACT

The purpose of this study was to compare three camera calibration approaches applied to underwater applications: (1) static control points with nonlinear DLT; (2) moving wand with nonlinear camera model and bundle adjustment; (3) moving plate with nonlinear camera model. The DVideo kinematic analysis system was used for underwater data acquisition. The system consisted of two gen-locked Basler cameras working at 100 Hz, with wide angle lenses that were enclosed in housings. The accuracy of the methods was compared in a dynamic rigid bar test (acquisition volume—$4.5 \times 1 \times 1.5$ m^3). The mean absolute errors were 6.19 mm for the nonlinear DLT, 1.16 mm for the wand calibration, 1.20 mm for the 2D plate calibration using 8 control points and 0.73 mm for the 2D plane calibration using 16 control points. The results of the wand and 2D plate camera calibration methods were less associated to the rigid body position in the working volume and provided better accuracy than the nonlinear DLT. Wand and 2D plate camera calibration methods presented similar and highly accurate results, being alternatives for underwater 3D motion analysis.

1. Introduction

The quantitative analysis of the 3D human motion is fundamental in different application domains, as sport science (Gourgoulis et al., 2008; Sarro and Barros, 2008; Machtsiras and Sanders, 2009; Miana et al., 2009), rehabilitation engineering (Lanini et al., 2008, Aliverti et al., 2001) and biomechanics (Figueroa et al., 2003; Chiari et al., 2005; Silvatti et al. 2009; Barros et al., 2010). Multi-camera systems (MVS) (BTS Engineering, Milan, Italy; Vicon, Oxford, UK) are largely used for indoor and laboratory measurements but their use outdoor or in constrained environments such as underwater for sport applications is still very limited. Among a number of critical issues preventing the straight application of the MVS to sport, the camera calibration procedure, which impacts on the system accuracy, is a crucial step. The camera calibration procedure involves the estimation of the intrinsic (focal length, distortion parameters, principal points, pixel scale factor) and extrinsic (location and orientation) parameters of each camera. In this paper, we focus on particular calibration methodologies allowing the MVS to be used in underwater applications, as sport performance evaluation and rehabilitation.

In underwater applications, large acquisition volumes are required and cumbersome calibration structure, having known geometry, based on a linear camera model (DLT—Direct Linear Transform), are commonly utilized (Gourgoulis et al., 2008; Machtsiras and Sanders, 2009). This camera model disregards the optical distortions that strongly impact the reconstruction accuracy. Better results were obtained when the optical distortion was modeled in the DLT method and a larger number of points were fixed to the calibration frame, as shown in Kwon, 1991. However, this implies in more control points on this cumbersome calibration structure (Kwon, 1991).

Two alternative approaches, wand-based and 2D plate-based, make use of simpler calibration objects and include nonlinear models for the camera. The wand-based approach consists of the static acquisition of a rigid structure, carrying the control points (CP), and the dynamic acquisition of the end point of a wand, which is moved within the field of view of the cameras. The DLT method was used to estimate the initial guess of the camera parameters, using the 2D/3D data coming from the known rigid structure, and on a nonlinear optimization to refine the parameters, based on the bundle adjustment approach, which uses the 2D data coming from the acquired wand (Fraser, 1997; Cerveri et al., 1998).

The 2D plate-based approach consists in the acquisition of a 2D plane in different positions and orientations. Similarly, it uses the DLT model to determine an initial guess of the parameters and

* Correspondence to: Universidade Estadual de Campinas, Faculdade de Educação Física, DEM, Laboratório de Instrumentação para Biomecânica, CX 6134, CEP 13083-851, Campinas, São Paulo, Brazil.
Tel.: +55 19 32516626; fax: +55 19 32894338.
E-mail address: amandasilvatti@yahoo.com.br (A.P. Silvatti).

0021-9290
doi:10.1016/j.jbiomech.2012.01.004

a nonlinear optimization for each camera separately to refine the parameters (Zhang, 2000).

Our aim was to compare these two calibration approaches with a previously proposed calibration approach based on static control points and a nonlinear form of the (radial and decentering optical distortion model) DLT method (Hatze, 1988), in terms of accuracy and flexibility in order to verify the relative advantages and disadvantages for underwater applications.

2. Methods

The DVideo kinematic analysis system, a multi-camera motion tracking system, was used in this study. The DVideo was developed by the present group for research applications in different areas such as biomechanics, image-based sport performance evaluation, human surface tracking and analysis (Figueroa et al. 2003, 2006; Barros, et al. 2006a,b; Sarro and Barros 2008; Miana et al., 2009; Sarro, et al., 2010; Barros et al., 2010; Lodovico et al., 2011). More recently, this system was applied in underwater data acquisition (Silvatti et al., 2009, 2010). Two gen-locked Basler cameras (Fig. 1D) working at 100 Hz, with wide angle lenses (8 mm focal length) enclosed in waterproof housings were adopted (Fig. 1A).

In order to perform the wand calibration, an orthogonal waterproof triad ($1\,m \times 1\,m \times 1\,m$) was built by a computer numerical control machine (CNC) screwing onto it nine spherical black markers (∅: 35 mm) in known positions (Fig. 1B). The 3D coordinates of the markers were known with accuracy of about 10 μm. The acquired markers were utilized to determine the initial guess of the camera parameters. The moving wand, carrying one marker at its end (Fig. 1B), was acquired in the whole working volume ($4.5 \times 1 \times 1.5\,m^3$) during 15 s. Two hundred and fifty useful frames were opportunely extracted from the whole sequence to refine the parameters by the bundle adjustment optimization, which uses CP with both known (triad markers) and unknown (wand marker) 3D coordinates. The bundle adjustment iteratively estimates the parameters of all the cameras along with the unknown 3D coordinates by minimizing the 2D projection error (measured vs. predicted by the camera model) on the image. The optical distortion was taken into account in the camera model, adopting a radial model with 2 parameters. In the wand calibration approach, the triad geometry provided the reference system (Fig. 1B).

In order to perform the 2D plate calibration, a waterproof chessboard (7×8 squares, 100×100 mm) was printed (300 dpi) and glued to a rigid planar support (Fig. 1C). The Zhang's approach (Zhang, 2000) was modified in this study using an additional rigid structure consisting in a graduated rod, equipped with four black markers, which was acquired in 4 different underwater positions. The water levels were measured in each graduated rod position to build the GCS with the water plane (Fig. 1D). The distances between the 4 positions of the graduated rod and the two points located on the swim pool border were measured to perform the triangulation and to obtain the CP 3D coordinates, which were used to compute the initial guess of the camera parameters. Two different amounts of CP (8 and 16) were utilized. The chessboard was moved by two persons in front of the two cameras assuming different positions and orientations spanning the entire working volume. The chessboard was moved at low speed (less than 25 cm/s, Fig. 1D). A corner is defined by the intersection of two black squares. Forty two corners were automatically detected in the images and tracked during the sequence. For parameter refinement, the acquisition was re-sampled to 10 Hz to obtain two hundred sequential frames. The optical distortion was taken into account in the camera model, adopting a radial and tangential model with 5 parameters.

The nonlinear DLT used the same 16 CP acquired for the 2D plate calibration and adopted the same distortion parameters in the camera model for the 2D plate too. In Table 1, we summarized the issues of the three camera calibration methods.

The accuracy of the calibration methods was assessed on the same 700 frames acquisition sequence of a rigid bar (two black markers) moved within the working volume and automatically tracked. The working volume was approximately the same in the three methods ($4.5 \times 1 \times 1.5\,m^3$) delimited at the middle of the swimming pool (Fig. 1D). The distance between markers (nominal value D: 291.89 mm) was obtained as a function of time (d_i). The following variables were calculated: (a) the mean absolute errors (MAE, Eq. (1)) (b) the standard deviation, (c) the minimum and (d) maximum error, (e) the root mean squared error (RMSE Eq. (2)) and (f) the RMSE relative to reconstruction expressed as a percentage of the real length of the rigid bar movement (Eq. (3)).

$$MAE = \frac{1}{N}\sum_{i}^{N} |d_i - D| \quad (1)$$

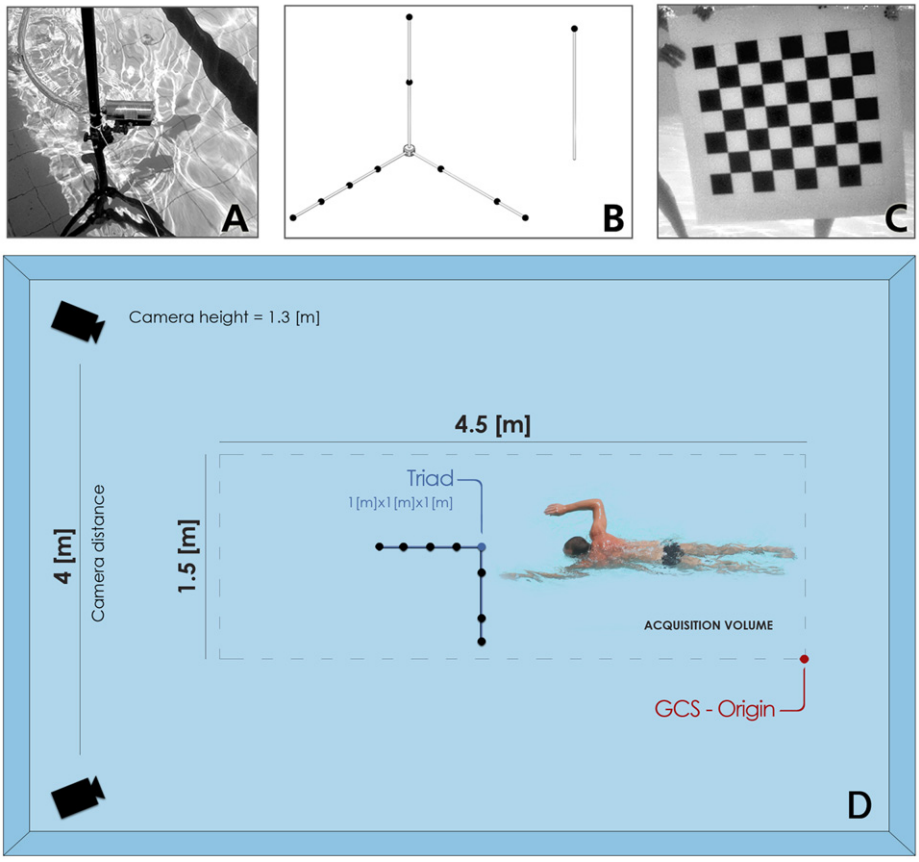

Fig. 1. (A) Camera enclosed in housings and fixed up tripods for underwater acquisition. (B) Triad and wand equipped with black markers used for wand calibration. (C) Chessboard used for 2D plate calibration. (D) Camera setup. The GCS was set on the water plane in the first position of the graduated rod (X – progression, Y – lateral displacement and Z – vertical).

$$\mathrm{RMSE} = \frac{1}{N}\sqrt{\sum_i^N (d_i - D)} \quad (2)$$

$$\%\mathrm{RMSE} = 100\frac{\frac{1}{N}\sqrt{\sum_i^N (d_i - D)^2}}{D} \quad (3)$$

3. Results

Table 2 shows the mean, standard deviation, minimum error, mean absolute errors, maximum error, RMSE of the distance curves between markers and the %RMSE for the nonlinear DLT, wand calibration and for both tests using the 2D plate calibration in the rigid bar test. The nonlinear DLT presented the worst results in all variables (Table 2 and Fig. 2A). The results of the wand calibration and 2D plate calibration (8 and 16 CP) were comparable in terms of MAE (1.16 mm, 1.20 mm, 0.73 mm). The mean values of the bar length and the mean absolute error for the 2D plate calibration with sixteen CP were better than those obtained in the configuration with eight CP, with the wand calibration and with the nonlinear DLT. However, the standard deviation (0.69 mm, 1.07 mm and 0.89 mm) and the maximum error (3.99 mm, 8.03 mm and 6.90 mm) were smaller in the wand calibration than in both 2D plate calibration configurations and nonlinear DLT.

Fig. 2A, B and C shows the error as function of frames and Fig. 2D, E and F show the influence of the rigid bar position in the acquisition volume on the error distribution for each camera calibration approach. Since increased error and a clear signal of the rigid bar movement can be seen related to the rigid bar position, we can assert that the nonlinear DLT was more affected by the movement of the rigid bar (Fig. 2A) and their position in the acquisition volume (Fig. 2D) than 2D plate calibration (Fig. 2B and E) and the wand calibration (Figs. 2C and F).

Table 1
Calibration methods.

Issues	Type of calibration		
	Nonlinear DLT	**Wand calibration**	**2D plate calibration**
Calibration support	Graduated rod	Triad + wand	Graduated rod + chessboard
Points to track	16 Spherical–black markers	Spherical–black markers	Planar–corners
Acquisition protocol	Graduated rod in 4 positions	Static triad + moving wand	Graduated rod in 4 positions + moving chessboard
Calibration approach	Least square method	DLT for initial guess Refinement by bundle adjustment	DLT for initial guess Refinement of the intrinsic parameters
	Single camera calibration	Camera network	Single camera calibration
Distortion model	Radial and tangential	Radial	Radial and tangential

Table 2
Results of the nonlinear DLT, the wand calibration, the 2D plate calibration using 8 points and the 2D plate calibration using 16 points in the dynamic test. Nominal value of the marker distance: 291.89 mm. The values are expressed in millimeters (mm).

	Mean	**Standard deviation**	**Minimum error**	**Mean absolute error**	**Maximum error**	**RMSE**	**%RMSE**
Nonlinear DLT	297.98	3.43	4.79	6.19	19.71	6.98	2.39
Wand calibration	290.77	0.69	0.20	1.16	3.99	1.31	0.45
2D plate calibration (8 CP)	292.87	1.07	0.19	1.20	8.03	1.45	0.50
2D plate calibration (16 CP)	291.67	0.89	0.07	0.73	6.90	0.92	0.31

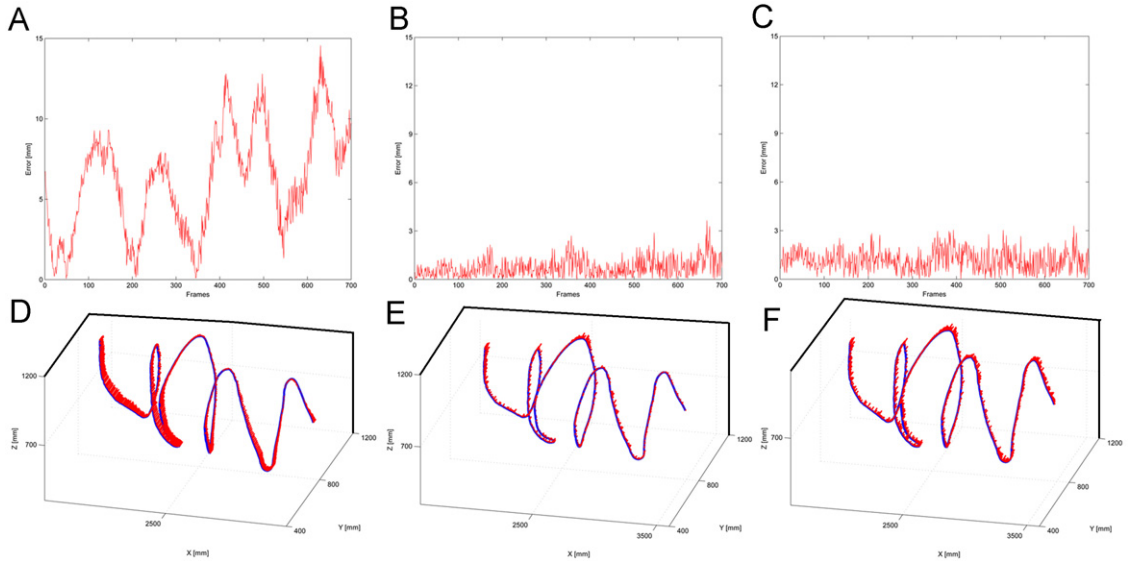

Fig. 2. Errors of the nonlinear DLT (A), 2D plate calibration (B) and wand calibration (C) as function of the acquisition frames. The distance error distribution over 700 frames of the testing bar and the error superimposed to one marker were displayed in (D)—nonlinear DLT, (E)—2D plate calibration and (F)—wand calibration.

Table 3
Synthesis of the advantages and disadvantages of the methods.

Type of calibration	Advantages	Disadvantages
Graduated rod+nonlinear DLT	• Just 16 markers in one frame to track • Allows to define a GCS aligned to water plane	• The rod setup is time consuming • Unbalanced camera network: each camera is calibrated separately. • Accuracy results related with the quantity of the CP • Increased error related to the acquisition position
Triad+wand calibration	• The triad setup is fast and easy • Only one point to track • Equalization of the reconstruction error across the calibration volume • High portability • Using two markers of known distance on the wand can better constraint the calibration	• The wand must be moved opportunely to cover all the calibration volume • Accuracy strictly depending of the construction of the triad • High sensibility of wand marker tracking to water quality • Assumes the vertical axis based on the swim pool floor
Graduated rod+2D plate calibration	• Easy corner tracking • More accurate distortion correction • Lower sensibility of corner detection to water • Allows to define a GCS aligned to water plane • Chessboard design and realization is straightforward	• The rod setup is time consuming • Unbalanced camera network: each camera is calibrated separately. • High number of corners to track • Rod and chessboard are cumbersome • Chessboard movement limitation to guarantee high detection accuracy and automatic corner labeling

4. Discussion and conclusion

In the wand method, just one marker was utilized because of the simplification of the tracking during the acquisition sequence. Commonly, commercial systems (BTS Engineering, Milan, Italy; Vicon, Oxford, UK) utilize two markers at the ends of the rigid bar including the marker distance as an additional constraint in the optimization. We envisage extending the use of the wand approach to two markers and updating the implementation of the bundle adjustment to include constraints about the marker distance. This could further increase the calibration accuracy.

According to the results, we can assert that the wand calibration allows a reduction (3.99 mm) of the error spread in the calibration volume. This is can be justified by the use of the bundle adjustment approach, which intrinsically tends to decrease the dispersion of the reconstruction error across all the calibration volume.

As far as 2D plate calibration is concerned, the distortion estimation exploited the virtual straight lines of the chessboard arguing that this led to better accuracy (0.73 mm). However, the accuracy results were slightly worse than previously found in similar setup (Silvatti et al., 2010). This fact might be due to the water transparency, which affects the 2D localization error that was better in the previous experiment. This suggests that the water transparency should be taken into account when highly accurate results are required. The use of the graduated rod allows the definition of the GCS aligned to the water level. While rod setup consumes more time than the triad, its use would be a technical advantage in two aspects: (1) allows to correct different depths in the swim pool; (2) provides the opportunity to deal with a geometrical axis that divides the swimmer motion task in underwater (positive) and out of water (negative). However, the rod setup is not so flexible and the use of the triad could be a valuable alternative measuring the water level with respect to it GCS.

The wand and 2D plate calibration methods (8 and 16 CP) led to underwater accuracy better than previously reported in the literature (MAE values of 5.12 mm were found in Yanai et al., 1996; RMS value of 5.6 mm and maximum error of 9.3 mm were detected in Kwon and Lindley, 2000; %RMS value of 1.28% was obtained in Gourgoulis et al., 2008; and RMS value of 5.2 mm was presented in Machtsiras and Sanders, 2009). It is well known that the number and the distribution of the CP strongly affect the DLT (Kwon and Lindley, 2000). This is true for the nonlinear DLT as well. Pribanić et al. (2008 and 2009) compared the wand and 2D plate camera calibration methods, but out of the water, and found MAE error distributions (5 calibration trials) ranging from 0.66 mm to 0.75 mm for the wand calibration and 0.69 mm to 0.84 mm for the 2D plate calibration, respectively. Our results were comparable to these values and with the accuracy of commercial systems used for dry land 3D analysis (Chiari et al., 2005).

The advantages and disadvantages of each method were synthesized in Table 3.

In conclusion we can summarize that the wand and 2D plate calibration approaches are promising alternatives for underwater 3D motion analysis. As far as sport performance measurement is concerned, future study involves the feasibility of moving stereo cameras for surveying the athletes during swimming tasks based on built-in calibration of the intrinsic parameters and rectilinear motion encoder to measure the extrinsic parameters.

Conflicts of interest statement

None.

Acknowledgments

Research supported by FAPESP (00/01293-1, 2006/02403-1 and 2009/09359-6), CNPq (473729/2008-3, 304975/2009-5) and CAPES (2011/10-7).

References

Aliverti, A., Dellacà, R., Pelosi, P., Chiumello, D., Gatihnoni, L., Pedoti, A., 2001. Compartmental analysis of breathing in the supine and prone positions by optoelectronic plethysmography. Annals of Biomedical Engineering 29 (1), 60–70.

Barros, R.M.L., Cunha, S.A., Magalhaes, W.J., Guimaraes, M.F., 2006a. Representation and analysis of soccer players'actions using principal components. Journal of Human Movement Studies 51, 103–116.

Barros, R.M.L., Russomanno, T.G., Figueroa, P.J., Brenzikofer, R., 2006b. A method to synchronise video cameras using the audio band. Journal of Biomechanics 39 (4), 776–780.

Barros, R.M.L, Menezes, R., Russomanno, T., Misuta, M., Brandao, B., Figueroa, P., Leite, N., Goldenstein, S., 2010. Measuring handball players trajectories using

an automatically trained boosting algorithm. Computer Methods in Biomechanics and Biomedical Engineering 14, 1–10.
Cerveri, P., Borghese, N.A., Pedotti, A., 1998. Complete calibration of a stereo photogrammetric system through control points of unknown coordinates. Journal of Biomechanics 31, 935–940.
Chiari, L., Croce, U.D., Leardini, A., Cappozzo, A., 2005. Human movement analysis using stereophotogrammetry, Part 2—Instrumental errors. Gait & posture 21, 197–211.
Figueroa, P.J., Leite, N.J., Barros, R.M.L., 2003. A flexible software for tracking of markers used in human motion analysis. Computer Methods and Programs in Biomedicine 72, 155–165.
Figueroa, P., Leite, N., Barros, R.M.L., 2006. Background recovering in outdoor image sequences: an example of soccer players segmentation. Image and Vision Computing 24 (4), 363–374.
Fraser, C.S., 1997. Digital camera self-calibration. ISPRS Journal of Photogrammetry and Remote Sensing 52, 149–159.
Gourgoulis, V., Aggeloussis, N., Kasimatis, P., Vezos, N., Boli, A., Mavromatis, G., 2008. Reconstruction accuracy in underwater three-dimensional kinematic analysis. Journal of Science and Medicine in Sport 11, 90–95.
Hatze, H., 1988. High-precision three-dimensional photogrammetric calibration and object space reconstruction using a modified DLT-approach. Journal,of Biomechanics 21, 533–538.
Kwon Y.H., Lindley S.L., 2000. Applicability of the localized-calibration methods in underwater motion analysis. In: Proceedings of the Sixteenth International Conference on Biomechanics in Sports; Hong Kong, China, pp. 48–55.
Kwon Y.H., 1991. Measurement for deriving kinematic parameters:numerical methods. In: Hong, Y., Barlet, R. (Eds.), Handbook of Biomechanics and Human Movement Science. Rooutledge, USA and Canada, pp. 156–181.
Lanini, B., Masolini, M., Bianchi, R., Binazzi, B., Romagnoli, I., Gigliotti, F., 2008. Chest wall kinematics during voluntary cough in neuromuscular patients. Respiration Physiology & Neurobiology 161 (1), 62–68.
Lodovico, A., Cerveri, P., Ferrigno, G., Barros, R.M.L., 2011. A novel video-based method using projected light to measure trunk volumes during respiration. Computer Methods in Biomechanical and Biomedical Engineering 14 (8), 707–713.
Machtsiras G., Sanders R.H., 2009. Accuracy of portable (PTZ digital) camera system designed for aquatic three-dimensional analysis. In: Proceedings of the 27th International Conference on Biomechanics in Sport; Limerick, Ireland, p. 451.
Miana, A.N., Prudêncio, M.V., Barros, R.M.L., 2009. Comparison of protocols for walking and running kinematics based on skin surface markers and rigid clusters of markers. International Journal of Sports Medicine 30 (11), 827–833.
Pribanić T., Sturm P., Cifrek M., 2008. Calibration of 3D kinematic systems using 2D calibration plate. In Proceedings of the 26th International Conference on Biomechanics in Sport; Seoul, Korea, pp. 77–80.
Pribanić, T., Sturm, P., Cifrek, M., 2009. A comparison between 2D plate calibration and wand calibration for 3D kinematic systems. Kinesiology 41, 147–155.
Sarro, K.J., Misuta, M., Burkett, B., Malone, L., Barros, R.M.L., 2010. Tracking of wheelchair rugby players in the 2008 demolition derby final. Journal of Sports Sciences 28, 193–200.
Sarro, K.J., Barros, R.M.L., 2008. Coordination between ribs motion and thoracoabdominal volumes in swimmers during respiratory maneuvers. Journal of Sports Science and Medicine 7, 195–200.
Silvatti A.P., Rossi M.M., Dias F.A.S., Leite N.J., Barros R.M.L., 2009. Non-linear camera calibration for 3D reconstruction using straight line plane object. In: Proceedings of the 27th International Conference on Biomechanics in Sport; Limerick, Ireland, p. 644.
Silvatti A.P., Telles T., Rossi M.M., Dias F.A.S., Leite N.J., Barros R.M.L., 2010. Underwater non-linear camera calibration: an accuracy analysis. In: Proceedings of the 28th International Conference on Biomechanics in Sport; Michigan, USA.
Yanai, T., Hay, J.G., Gerot, J.T., 1996. Three-dimensional videography of swimming with panning periscopes. Journal of Biomechanics 29, 673–678.
Zhang, Z., 2000. A flexible new technique for camera calibration. IEEE Transactions on Pattern Analysis and Machine Intelligence 22, 1330–1334.